Controller Design Optimization of a Multi-DOF System Using Response Optimizer Toolbox

Saliha KÖPRÜCÜ
Necmettin Erbakan University

Engin Hasan ÇOPUR
Necmettin Erbakan University

Hasan Huseyin BILGIC
Necmettin Erbakan University

To Cite This Chapter

Köprücü, S., Çopur, E. H., & Bılgıc, H. H. (2024). Controller Design Optimization of a Multi-DOF System Using Response Optimizer Toolbox. In S. Koçer & Ö. Dündar (Eds.), *Intelligent Systems and Optimization in Engineering* (pp. 67-79). ISRES Publishing.

Introduction

Control applications for multi-degree-of-freedom (multi-DOF) systems play a crucial role today, especially in the stabilization and guidance of complex dynamic systems such as aircraft. In this context, the modeling, simulation, and control of multi-DOF systems are frequently addressed in both academic research and industry. Studies on these systems provide engineering students and researchers with in-depth knowledge of dynamic system control, while also enabling engineers to apply this knowledge in real-world applications. This section discusses the use of MATLAB/Simulink Response Optimizer, an effective tool for controlling multi-DOF systems, and explains the design of a controller for a multi-DOF system.

A review of the literature reveals that optimal controllers are often used in the control of multi-DOF systems when specific performance criteria, such as energy consumption, error rate, response time, or stability, need to be optimized (Hassaan 2021; Ekinci et al. 2021; İzci et al. 2021). However, constraining the control responses of these systems to a desired range often requires precise tuning. To achieve this, artificial intelligence algorithms are usually preferred for fine-tuning (Bilgic et al. 2016; Bilgic et al. 2021). At this stage, designing a multi-objective function, which requires expertise, becomes necessary (Rodríguez-Molina et al. 2020). For these reasons, MATLAB/Simulink's Response Optimizer stands out as an effective tool for adjusting the controller parameters of multi-DOF systems under specific constraints (Azeez et al. 2023).

Mahmoud and AlRamadhan (2021) examined two different SMC controller structures with the aim of achieving smooth transient and robust steady-state responses to track the reference rotor position when the hybrid stepper motor is subjected to load disturbances. They optimized the controller parameters using Simulink Response Optimizer application. Lachekhab et al. (2022), in their study on creating an accurate mathematical model of a quadcopter, controlled the position and attitude of the

quadcopter in three-dimensional space. For this purpose, roll, pitch, and yaw angles, as well as altitude and position, were all controlled using SMC. They also used the Simulink Response Optimizer tool to optimize several control parameters in the SMC controller design. Wu et al. (2023) proposed a modeling and tracking control strategy based on fractional calculus to achieve high-accuracy control of dielectric elastomer actuators (DEAs). Since tracking control accuracy depends on the controller parameters, they applied a two-stage optimization process to optimize the FFCC parameters. In the first stage, the controller parameters were optimized based on a reduced-order model of the DEA using a gradient descent algorithm and Simulink's Response Optimizer application in the simulation environment. Following this, the control experiment was conducted, with root-mean-square errors in the experiment all recorded below 0.7%.

Gopi et al. (2023) introduced a new optimization technique, Simulink Design Optimization (SDO), for calculating optimal PID coefficients in automatic voltage regulators (AVRs). In their study, the performance of the SDO-PID controller is compared to PID controllers using water cycle algorithms, genetic algorithms, and local unimodal sampling algorithms. Results demonstrate that the SDO-PID controller, utilizing the response optimizer, not only outperforms traditional methods but also provides a broader stability range. This makes it a promising solution for enhancing the efficiency and reliability of automatic voltage regulation systems, contributing to more effective voltage management in various applications. In a study aimed at developing more efficient, robust, and user-friendly teleoperation systems, Nour et al. (2023) optimized the controller and parameter set in two bilateral teleoperation control schemes using the Simulink Response Optimizer tool. They performed a comparative analysis of each architecture's performance in terms of transparency and stability, considering both constant and variable time delays. The response optimizer tool was used to obtain the best set of tuning parameters that optimized the specified objective function and, in this case, minimized the tracking position error between master and slave devices.

Alhattab et al. (2023) used a controller called D-STATCOM to reduce voltage fluctuations in electrical power systems. In their study, they developed an AI-based control system with fuzzy logic and ANFIS to achieve faster, more stable control compared to the conventional PI controller. The gain parameters of the PI controller were optimized using Simulink Response Optimizer tool, enabling the system to adapt more quickly to varying load conditions. This approach effectively restored voltage to its nominal value during voltage sag and swell events, with simulation results demonstrating the success of the optimization-supported control system in enhancing power quality.

Example Study: As an example application, a Quanser 3DOF Hover system with three degrees of freedom was tested (Figure 1).

Figure 1

Quanser 3DOF Hover System (Quanser, 2024)

The Quanser 3DOF Hover system is a platform capable of movement in three axes (roll, pitch, and yaw) (Quanser, 2024). It is an ideal experimental system designed to test various control theories. The system's three-degree-of-freedom movement capability offers a significant advantage for simulating guidance and stabilization problems, especially for unmanned aerial vehicles (UAVs). The 3DOF Hover system consists of a motorized propeller mechanism and a platform that allows free rotation along three axes. The primary objective of the system is to develop a suitable control algorithm to maintain specific angular positions stably. Controlling this type of system is challenging from an engineering perspective due to its non-linear dynamics, making the 3DOF Hover system valuable for both educational and research purposes (Quanser, 2024).

Anna Prach et al. evaluated the control performance of nonlinear systems using the forward propagating Riccati equation (FPRE) and linear-quadratic regulator (LQR) methods in their paper. FPRE provides more flexible and effective control over a wider operating range by updating feedback gains in real time. In experiments conducted on the Quanser 3DOF Hover test system, FPRE demonstrated superior performance compared to LQR, particularly in handling high-amplitude commands. The study shows that FPRE offers a more robust control approach for nonlinear systems. Fethi Ouerdane et al. (2024) aimed to test the visual servoing systems of low-cost UAVs using Quanser's 3DOF hover quadcopter in an indoor environment without GPS. The system reads commands specified by QR codes and processes positional information using LabVIEW and hardware-in-the-loop (HIL) simulation. It employs PID controllers for horizontal and vertical position tracking and uses the LQR algorithm for roll, pitch, and yaw control. In the experiments, the Quanser quadcopter successfully performed positioning and tracking via QR codes, maintaining its tracking capability despite some detection limitations. The results indicate that this method can be adapted for advanced applications such as asset tracking and indoor inspections with 6-DOF UAVs. Normann (2023) investigated event-triggered (ETC) and self-triggered (STC) control strategies on the Quanser 3DOF Hover system to conserve energy and processing power in resource-constrained control systems. ETC continuously monitors the state of the Quanser hover system and updates only when necessary, while STC conserves energy by establishing a predictive update schedule. Simulations and experiments showed that the ETC strategy successfully maintained stability in the real system, while STC was more sensitive to modeling errors and external disturbances. It was found that ETC improved energy and bandwidth efficiency while keeping the Quanser hover system stable, whereas STC performed well in simulations but did not meet expectations in real-world applications.

Mathematical Modelling of 3Dof Hower System

Free-Body Diagram of the System

To perform a valid simulation, the created system must be accurately represented in the computer environment. Achieving this requires that the mathematical model of the system closely reflects reality. A mathematical model, in its simplest form, is a representation of a real system, whether planned or already existing, using only mathematical expressions. In the process of mathematical modeling, fundamental physical laws are employed to translate the real-world problem into a mathematical framework.

When dealing with a nonlinear system, as in this study, achieving a highly accurate mathematical model becomes challenging. Consequently, certain assumptions are made, and the system is linearized as much as possible to obtain an accurate model. Below are some of the assumptions made during the modelling process:

- The 3-DOF hover experiment set is rigid and symmetrical.
- The center of gravity of the 3-DOF hover experiment set is at the intersection of the

X, Y, and Z axes.

- The motors of the experiment set are rigidly fixed to the body.
- The experiment set is parallel to the ground when the pitch and roll angles are zero $(\theta_p = 0, \theta_r = 0)$.
- When the body of the experiment set rotates counterclockwise, the yaw angle increases.
- When the experiment set rotates counterclockwise around the Y-axis, the pitch angle increases.
- When the experiment set rotates clockwise around the X-axis, the roll angle increases.

The free-body diagram of the isometric view of the 3-DOF hover experiment set used in this study's simulation files is shown in Figure 2, along with the positive rotation directions of the X-Y-Z axes, defined respectively as the Roll-Pitch-Yaw axes.

Figure 2

Free-Body Diagram of the Isometric View of the 3DOF Hover Experimental Set

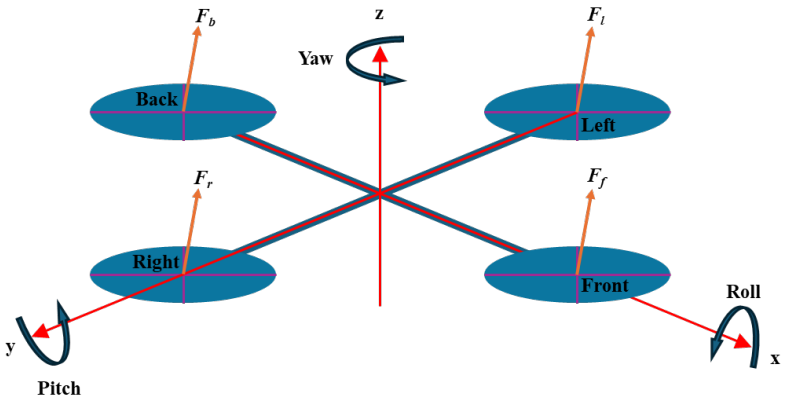

The 3-DOF hover experiment set has four DC motors positioned at the front, back, right, and left, as illustrated in Figure 2. When a positive voltage is applied to these motors, they provide the thrust required to activate the system. The thrust generated by these motors is denoted as F_f, F_b, F_r and F_l respectively.

Pitch, Roll and Yaw-Axis Model of the System

The motors placed at the front and back are primarily responsible for controlling the pitch angle. When the thrust generated by the front motor exceeds that of the back motor, the pitch angle increases $(F_f > F_b)$.

Figure 3 provides a free-body diagram of this scenario:

Figure 3

Free-Body Diagram of the 3DOF Hover Experimental Set Viewed from the Right Side

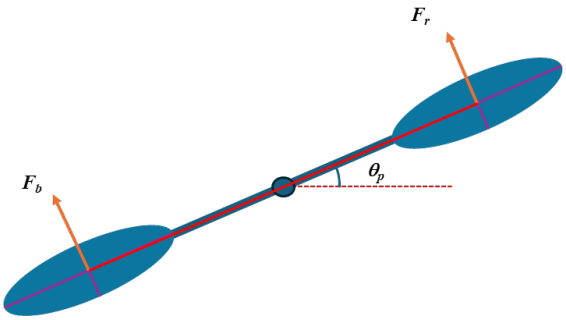

The general equation for the dynamics of each axis is described as follows:

$$J\ddot{\theta} = \Delta FL \tag{1}$$

where J is the moment of inertia with respect to the axis, $\ddot{\theta}$ is the angular acceleration, ΔF is the differential thrust force, and L is the distance of the motor from the centre.

When Equation (1) is applied to the system's free-body diagram shown in Figure 3, the following equation is obtained:

$$J_p\ddot{\theta}_p = K_f(V_f - V_b) \tag{2}$$

where K_f is the thrust force constant, V_f and V_b are the voltages supplied to the front and back motors, respectively, θ_p is the pitch angle, and J_p is the moment of inertia about the Y-axis (pitch-axis).

Similarly, for the X-axis (roll-axis), we have:

$$J_r\ddot{\theta}_r = K_f(V_r - V_l) \tag{3}$$

where V_r and V_l are the voltages supplied to the right and left motors, θ_r is the roll angle, and the J_r is the moment of inertia about the roll-axis. These equations describe the movements in the roll and pitch axes, while the yaw axis differs from these two.

Figure 4

Free-Body Diagram of the Top View of the 3DOF Hover Experimental Set

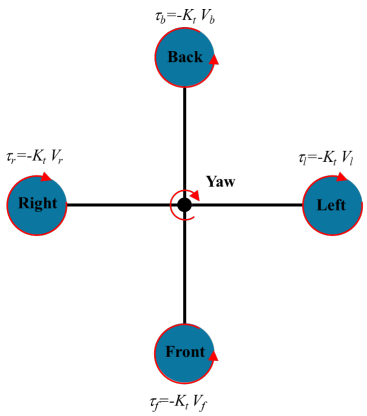

As shown in Figure 4, opposite motors rotate in the same direction, while consecutive motors rotate in opposite directions. Since the motors are equidistant from the centre, this design symmetry maintains force and moment balance. To initiate motion along the Z-axis (yaw axis), this balance must be disrupted. The equation for motion in the yaw axis is given as follows:

$$J_y\ddot{\theta}_y = \Delta\tau = \tau_l + \tau_r - \tau_f - \tau_b \tag{4}$$

where τ_l and τ_r are the torques generated by the clockwise-rotating propellers on the left and right, respectively, and τ_f and τ_b are the torques generated by the counterclockwise-rotating propellers at the front and back. Letting K_t be the thrust-torque constant and V_m the motor voltage, the total torque generated by all propellers can be represented as:

$$\tau = K_t V_m \tag{5}$$

Thus, the yaw-axis equation of motion can be written as:

$$J_y\ddot{\theta}_y = K_t(V_r + V_l) - K_t(V_f + V_b) \tag{6}$$

State-Space Model of the System

To apply the Linear Quadratic Regulator (LQR) method to the system, whose equations of motion are given in the previous section, the system's state-space model must be derived. As we know, the general representation of a state-space model can be written as:

$$\begin{aligned} \dot{x} &= Ax + Bu \\ y &= Cx + Du \end{aligned} \tag{7}$$

where x represents the state variable. The state vector of the 3DOF hover experiment set is as follows:

$$x^T = \begin{bmatrix} \theta_y & \theta_p & \theta_r & \dot{\theta}_y & \dot{\theta}_p & \dot{\theta}_r \end{bmatrix} \tag{8}$$

The output vector of the 3DOF hover experiment set is as follows:

$$y^T = \begin{bmatrix} \theta_y & \theta_p & \theta_r \end{bmatrix} \tag{9}$$

The control vector of the 3DOF hover experiment set is as follows:

$$u^T = \begin{bmatrix} V_f & V_b & V_r & V_l \end{bmatrix} \tag{10}$$

Using the equations of motion given above, the state-space matrices are defined as follows:

$$A=\begin{bmatrix}0&0&0&1&0&0\\0&0&0&0&1&0\\0&0&0&0&0&1\\0&0&0&0&0&0\\0&0&0&0&0&0\\0&0&0&0&0&0\end{bmatrix},$$

$$B=\begin{bmatrix}0&0&0&0\\0&0&0&0\\0&0&0&0\\-K_t/J_y&-K_t/J_y&K_t/J_y&K_t/J_y\\LK_f/J_p&-LK_f/J_p&0&0\\0&0&LK_f/J_r&-LK_f/J_r\end{bmatrix},$$

$$C=\begin{bmatrix}1&0&0&0&0&0\\0&1&0&0&0&0\\0&0&1&0&0&0\end{bmatrix},$$

$$D=\begin{bmatrix}0&0&0&0\\0&0&0&0\\0&0&0&0\end{bmatrix}.$$

$$\begin{bmatrix}\dot{\theta}_y\\\dot{\theta}_p\\\dot{\theta}_r\\\ddot{\theta}_y\\\ddot{\theta}_p\\\ddot{\theta}_r\end{bmatrix}=\begin{bmatrix}0&0&0&1&0&0\\0&0&0&0&1&0\\0&0&0&0&0&1\\0&0&0&0&0&0\\0&0&0&0&0&0\\0&0&0&0&0&0\end{bmatrix}\begin{bmatrix}\theta_y\\\theta_p\\\theta_r\\\dot{\theta}_y\\\dot{\theta}_p\\\dot{\theta}_r\end{bmatrix}+\begin{bmatrix}0&0&0&0\\0&0&0&0\\0&0&0&0\\-K_t/J_y&-K_t/J_y&K_t/J_y&K_t/J_y\\LK_f/J_p&-LK_f/J_p&0&0\\0&0&LK_f/J_r&-LK_f/J_r\end{bmatrix}\begin{bmatrix}V_f\\V_b\\V_r\\V_l\end{bmatrix} \tag{11}$$

$$\begin{bmatrix}\theta\\\theta\\\theta\end{bmatrix}=\begin{bmatrix}1&0&0&0&0&0\\0&1&0&0&0&0\\0&0&1&0&0&0\end{bmatrix}\begin{bmatrix}\theta\\\theta\\\theta\\\dot{\theta}\\\dot{\theta}\\\dot{\theta}\end{bmatrix}+\begin{bmatrix}0&0&0&0\\0&0&0&0\\0&0&0&0\end{bmatrix}\begin{bmatrix}\\\\\\\end{bmatrix} \tag{12}$$

Optimisation Process by Using Response Optimizer Toolbox

MATLAB/Simulink Response Optimizer Toolbox

The MATLAB System Optimizer Toolbox allows engineers and researchers to improve performance by optimizing system parameters. This toolbox aims to automatically adjust the control parameters of complex systems to achieve the desired performance. In control systems, manual tuning of dynamic parameters is often time-consuming and prone to error. By providing precise parameter optimization, this toolbox accelerates the tuning process.

The toolbox allows users to define cost functions and constraints to set optimization objectives. For example, cost functions can be created based on criteria such as minimizing the system's settling time or ensuring that an output signal converges to a specific value. MATLAB uses different optimization algorithms to determine the optimal parameters based on these criteria.

The compatibility of the toolbox with Simulink enables users to directly perform optimization on Simulink models. This functionality makes it possible to automatically optimize control system parameters and view the results graphically. For instance, in designing a PID controller, the PID gains can be optimized using the System Optimizer Toolbox to enhance system stability. With comprehensive analysis and simulation capabilities, the MATLAB Response Optimizer Toolbox is a powerful tool that increases efficiency in fields such as control engineering and system analysis.

Case Study: Tuning of LQR State Weighting Matrix Gains

As an example application, the control block diagram of the Quanser 3DOF Hover system is presented in Figure 5.

Figure 5

Control Block Diagram of Quanser 3DOF Hover System (Quanser, 2024)

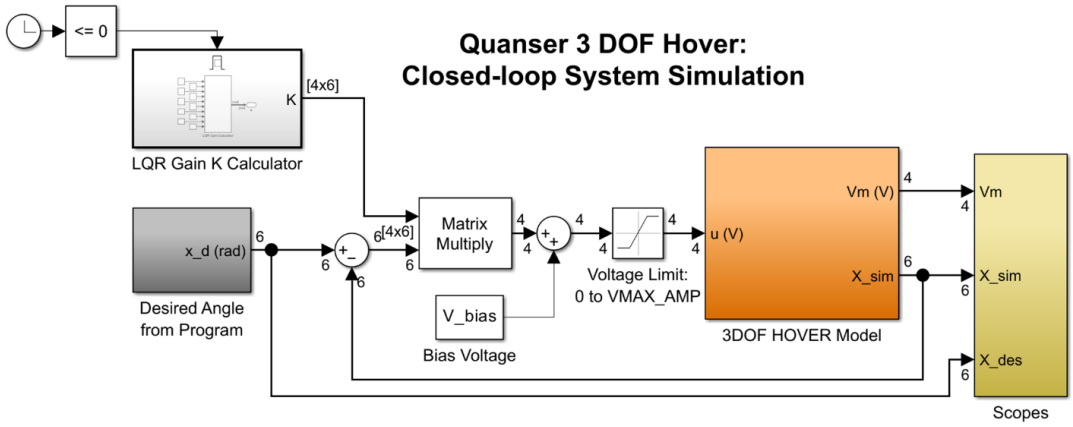

The controller's gains based on the state-space model are determined by adjusting the weighting matrices using the Response Optimizer Toolbox. The ten parameters of the Q and R matrices, shown in Equation 13 as $q1$, $q2$, $q3$, $q4$, $q5$, $q6$, $r1$, $r2$, $r3$, and $r4$, are adjusted to meet the response requirements.

$$Q = \begin{bmatrix} q_1 & 0 & 0 & 0 & 0 & 0 \\ 0 & q_2 & 0 & 0 & 0 & 0 \\ 0 & 0 & q_3 & 0 & 0 & 0 \\ 0 & 0 & 0 & q_4 & 0 & 0 \\ 0 & 0 & 0 & 0 & q_5 & 0 \\ 0 & 0 & 0 & 0 & 0 & q_6 \end{bmatrix},$$

$$R = \begin{bmatrix} r_1 & 0 & 0 & 0 \\ 0 & r_2 & 0 & 0 \\ 0 & 0 & r_3 & 0 \\ 0 & 0 & 0 & r_4 \end{bmatrix} \tag{13}$$

When tuning the controller parameters with the Response Optimizer Toolbox, the following steps are applied in sequence:

- The variables to be adjusted are defined symbolically in Simulink.
- A response envelope is created for the variables to be controlled in the output.
- A set of design variables is specified, with lower and upper limits set if applicable.
- The optimization process is initiated.

The optimization then proceeds using the gradient descent approach until the conditions fall within the response envelope. If conditions are not met, the optimization process automatically stops upon reaching the predetermined number of iterations.

Figure 6
MATLAB/Simulink Response Optimizer Toolbox

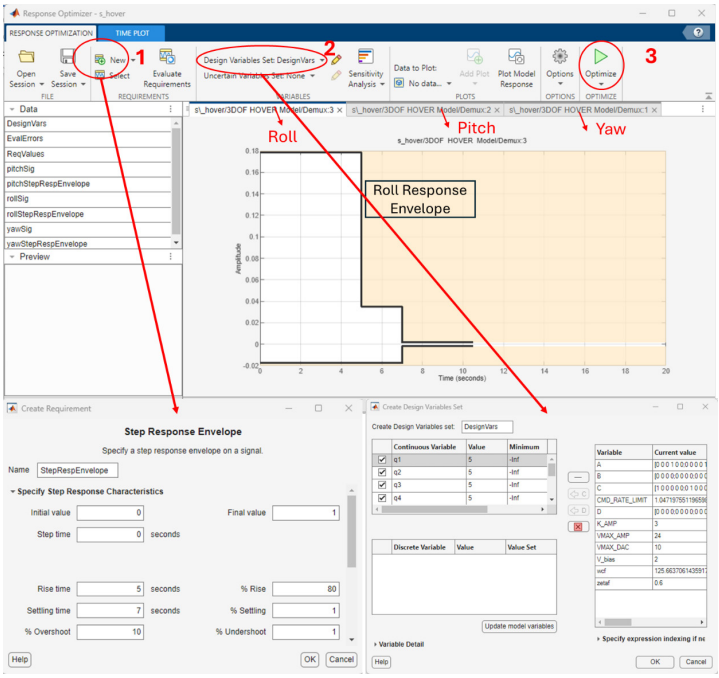

Results

In this study, fine-tuning of the weighting matrices for the LQR controller was conducted for a regulator problem. The objective of the regulator problem is to control the transition of a four-rotor system from specified pitch, roll, and yaw angles to a hover position. The system's initial conditions are set as , $\theta_p(0) = 10°$ and $\theta_y(0) = 20°$. To achieve precise tuning of the LQR controller's weighting matrices, constraints on the time response envelope for each rotational axis were specified as follows: a rise time of 5 seconds, a settling time of 7 seconds, a maximum overshoot of 10%, and a steady-state error within ±1%. Based on these constraints, the optimized Q and R matrices were determined as follows:

$$Q = \begin{bmatrix} 23.433 & 0 & 0 & 0 & 0 & 0 \\ 0 & 10.191 & 0 & 0 & 0 & 0 \\ 0 & 0 & 36.484 & 0 & 0 & 0 \\ 0 & 0 & 0 & 21.825 & 0 & 0 \\ 0 & 0 & 0 & 0 & 4.7375 & 0 \\ 0 & 0 & 0 & 0 & 0 & 3.246 \end{bmatrix} \tag{14}$$

$$R = \begin{bmatrix} 3.225 & 0 & 0 & 0 \\ 0 & 3.811 & 0 & 0 \\ 0 & 0 & 4.3816 & 0 \\ 0 & 0 & 0 & 3.488 \end{bmatrix} \tag{15}$$

The simulation results for the system's pitch, roll, and yaw angle responses over time, obtained using these optimized Q and R matrices, are shown in Figure 7. The results indicate that the system successfully transitioned to the hover position while meeting the defined time response constraints.

Figure 7

Controller Responses Under Initial Angular Positions

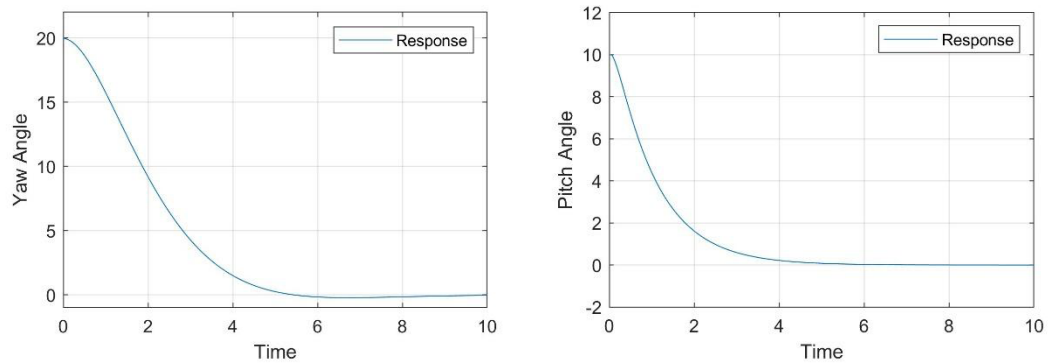

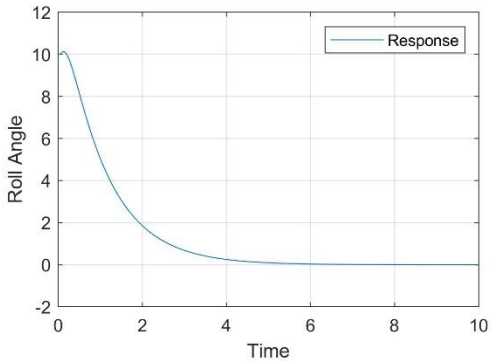

Additionally, another simulation was conducted to evaluate the performance of the optimized control parameters in reference tracking. In this simulation, the objective was for the system to follow predetermined square trajectories for each rotational angle. The square wave inputs were set as follows: an amplitude of 4 degrees and a frequency of 0.08 Hz for the roll angle, an amplitude of 4 degrees and a frequency of 0.1 Hz for the pitch angle, and an amplitude of 5 degrees and a frequency of 0.04 Hz for the yaw angle. The results are presented in Figure 8. The simulation results indicate that the optimized controller successfully tracked each reference input in all three axes.

Figure 8

Controller Responses for Square Trajectories

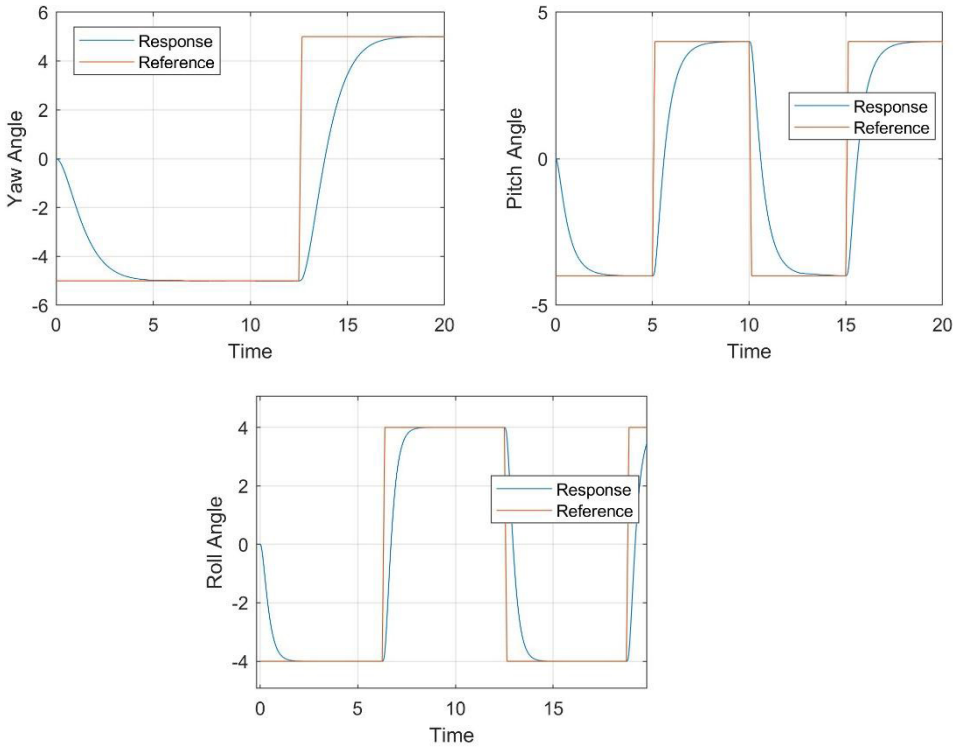

Conclusion

In this study, the effectiveness of the MATLAB/Response Optimizer Toolbox in solving control problems for multi-degree-of-freedom systems was examined. Since dynamic systems are often structured with multiple degrees of freedom, designing controllers for these systems poses various challenges. Precise tuning of control parameters is especially crucial for successfully meeting control criteria. The MATLAB/ Response Optimizer Toolbox provides an effective method for addressing these issues in

multi-degree-of-freedom systems.

This study offers foundational information on using the MATLAB/Response Optimizer Toolbox and demonstrates its application to a control problem, providing users with practical insights. Furthermore, based on the results obtained from the control application in this study, it has been shown that control parameters can be successfully optimized according to control design criteria.

References

Alhattab, A. S., Alsammak, A. N. B., & Mohammed, H. A. (2023). An intelligent mitigation of disturbances in electrical power system using distribution static synchronous compensator. *Indonesian Journal of Electrical Engineering and Computer Science*, *30*(2), 633-642.

Azeez, M. I., Abdelhaleem, A. M. M., Elnaggar, S., Moustafa, K. A., & Atia, K. R. (2023). Optimized sliding mode controller for trajectory tracking of flexible joints three-link manipulator with noise in input and output. *Scientific reports*, *13*(1), 12518.

Bilgic, H. H., Sen, M. A., & Kalyoncu, M. (2016). Tuning of LQR controller for an experimental inverted pendulum system based on The Bees Algorithm. *Journal of Vibroengineering*, *18*(6), 3684-3694.

Bilgic, H. H., Sen, M. A., Yapici, A., Yavuz, H., & Kalyoncu, M. (2021). Meta-heuristic tuning of the LQR weighting matrices using various objective functions on an experimental flexible arm under the effects of disturbance. *Arabian Journal for Science and Engineering*, *46*(8), 7323-7336.

Ekinci, S., Izci, D., & Hekimoğlu, B. (2021). Optimal FOPID speed control of DC motor via opposition-based hybrid manta ray foraging optimization and simulated annealing algorithm. *Arabian Journal for Science and Engineering*, *46*(2), 1395-1409.

Gopi, P., Srinivasa Varma, P., Sai Kalyan, C. N., Ravikumar, C. V., Srinivasulu, A., Bohara, B., ... & Sathish, K. (2023). Dynamic behavior and stability analysis of automatic voltage regulator with parameter uncertainty. *International Transactions on Electrical Energy Systems*, *2023*(1), 6662355.

Hassaan, G. A. (2021). Tuning of a PD-PI Controller to Control Overdamped Second-Order-Like Processes. *Journal homepage: www. ijrpr. com ISSN*, *2582*, 7421.

Izci, D., Ekinci, S., Kayri, M., & Eker, E. (2022). A novel improved arithmetic optimization algorithm for optimal design of PID controlled and Bode's ideal transfer function based automobile cruise control system. *Evolving Systems*, *13*(3), 453-468.

Lachekhab, F., Zamoum, R. B., Belatreche, R., Kouzou, A., & Acheli, D. (2022, May). Modified Sliding Mode Control of Autonomous Quadrotor. In *2022 19th International Multi-Conference on Systems, Signals & Devices (SSD)* (pp. 1248-1254). IEEE.

Mahmoud, M. S., & AlRamadhan, A. H. (2021). Optimizing the parameters of sliding mode controllers for stepper motor through Simulink response optimizer application. *International Journal of Robotics and Control Systems*, *1*(2), 209-225.

Normann, V. (2023). *Event-triggered and self-triggered control of a 3 DOF hover system* (Master's thesis, uis).

Nour, M., Farid, F., & Adel, O. (2023, October). Optimizing Bilateral Teleoperation Control Architectures: A Comparative Study Under Constant and Variable Time Delays. In *2023 International Conference on Networking and Advanced Systems*

(ICNAS) (pp. 1-6). IEEE.

Ouerdane, F., & Mysorewala, M. F. (2024, June). Visual Servoing of a 3 DOF Hover Quadcopter using 2D Markers. In *2024 IEEE 33rd International Symposium on Industrial Electronics (ISIE)* (pp. 1-6). IEEE.

Quanser 3 DoF Hover - Flight Dynamics and Control of Vertical Lift-off Vehicles. Quanser, 2024. URL https://www.quanser.com/products/3-dof-hover/. Accessed 04 October 2024.

Prach, A., Kayacan, E., & Bernstein, D. S. (2016, July). An experimental evaluation of the forward propagating Riccati equation to nonlinear control of the Quanser 3 DOF Hover testbed. In *2016 American Control Conference (ACC)* (pp. 3710-3715). IEEE.

Rodríguez-Molina, A., Mezura-Montes, E., Villarreal-Cervantes, M. G., & Aldape-Pérez, M. (2020). Multi-objective meta-heuristic optimization in intelligent control: A survey on the controller tuning problem. *Applied Soft Computing*, *93*, 106342.

Wu, J., Xu, Z., Zhang, Y., Su, C. Y., & Wang, Y. (2023). Modeling and tracking control of dielectric elastomer actuators based on fractional calculus. *ISA transactions*, *138*, 687-695.

About the Authors

Saliha KÖPRÜCÜ graduated from the Department of Aeronautical Engineering at Necmettin Erbakan University, located in Konya, in 2023, and subsequently began her master's studies in the same department. She is currently continuing her graduate studies and has been working as a research assistant at Necmettin Erbakan University since December 2023. Her research areas include Aerospace Vehicle Dynamics, Control, and Autonomous Systems, in which she aims to gain expertise.
E-mail: salihakoprucu@gmail.com, **ORCID:** 0009-0007-9685-0008

Engin Hasan ÇOPUR gradauted as a mechanical engineer in 2007 from Gazi University which is located in Ankara, the capital city of Türkiye. Then started my MSc study in the same university and completed it in 2011. During this period, the author was also working as a research assistant there. After completing MSc study, author was able to obtain a state funding for my PhD study in UK and gained a Phd position in University of Southampton. Then author returned Turkey and started working as a lecturer in 2017 in Necmettin Erbakan University which is located in Konya Türkiye. Since 2017, author held the same position.
E-mail: engincopur@gmail.com, **ORCID:** 0000-0003-0837-1255

Hasan Huseyin BILGIC is received MSc. from Department of Mechanical Engineering, Mustafa Kemal University, Hatay, Turkey, in 2014 and then received PhD from Department of Mechanical Engineering, İskenderun Technical University, Hatay, Turkey, in 2018. Now he is Assistant Professor at Department of Aeronautical Engineering, Necmettin Erbakan University, Konya, Turkey. His current research interests include command/input shaping, sliding mode control, artificial intelligence, linear and nonlinear control systems, UAV system design and control.
E-mail: bilgichh@gmail.com, **ORCID:** 0000-0001-6006-8056

Similarity Index
The similarity index obtained from the plagiarism software for this book chapter is 13%.